

Thermal Distribution in Axial-Flow Fixed Bed with Flowing Gas

Kun Lei, Hongfang Ma, Haitao Zhang, Weiyong Ying, and Dingye Fang

Abstract—This paper reported an experimental research of steady-state heat transfer behaviour of a gas flowing through a fixed bed under the different operating conditions. Studies had been carried out in a fixed-bed packed methanol synthesis catalyst percolated by air at appropriate flow rate. Both radial and axial direction temperature distribution had been investigated under the different operating conditions. The effects of operating conditions including the reactor inlet air temperature, the heating pipe temperature and the air flow rate on temperature distribution was investigated and the experimental results showed that a higher inlet air temperature was conducive to uniform temperature distribution in the fixed bed. A large temperature drop existed at the radial direction, and the temperature drop increased with the heating pipe temperature increasing under the experimental conditions; the temperature profile of the vicinity of the heating pipe was strongly affected by the heating pipe temperature. A higher air flow rate can improve the heat transfer in the fixed bed. Based on the thermal distribution, heat transfer models of the fixed bed could be established, and the characteristics of the temperature distribution in the fixed bed could be finely described, that had an important practical significance.

Keywords—Thermal distribution, heat transfer, axial-flow, fixed bed.

I. INTRODUCTION

METHANOL shows great advantages in properties, economy and its practical application as an alternative fuel [1]. Large scale methanol synthesis is the trend of the methanol industry in the world and corresponding methanol synthesis reactor technology is necessary for large scale methanol production [2]. Fixed-bed, due to their high surface

area-to-volume ratio is widely used in the chemical and process industries as reactors, ion exchange columns and absorption towers [3]. Especially the randomly packed bed reactors, because of their low cost and ease of use compared to other packing methods, are often used in applications in which the need for the removal of heat from highly-exothermic chemical reactions (e.g., methanol synthesis from syngas). Randomly packed beds will most probably remain the “default” catalytic reactor for at least a few more decades, mainly because of their advantages above [4].

Heat transfer can play a crucial role in determining the performance of such devices and has therefore been a subject of numerous investigations over the past few decades. Many papers have been published on heat transfer in fixed bed approaching several facets of this subject.

Single phase reacting flows in a randomly packed bed reactor were investigated by Freund et al. [5] with LBM method.

Stefan et al. [6] developed a composite heat transfer correlation for saturated flow boiling in small channels, which includes nucleate boiling and convective heat transfer terms while accounting for the effect of bubble confinement in small channels.

Dixon et al. [7] simulated the heat transfer in fixed beds of spheres via established CFD models, and validated by comparison to experimental measurements in a pilot-scale rig. The agreement between CFD simulations and experimental data was very satisfactory.

Guardo et al. [8], studied two different configurations: forced convection at low pressure (with air as circulating fluid) and mixed convection at high pressure (with supercritical CO₂ as circulating fluid), and then compared the numerical data with the previously published data. They obtained a novel CFD-based correlation for free, forced and mixed convection at high pressure.

Calis et al. [9] used a commercial CFD code to predict the pressure drop characteristics of packed beds of spheres that have a channel-to-particle-diameter ratio of 1.00 to 2.00, with an average error of about 10%, and this error is acceptable for design purposes.

Jian Xu et al. [10] have studied the detailed axial temperature distribution in a two-stage process for catalytic partial oxidation of methane to syngas, and found that both oxygen splitting ratio and gas hourly space velocity (GHSV) have significant influence on the temperature profile in the reactor.

Jianmin Wu et al. [11] investigated the thermal conductivity

K. Lei is with Engineering Research Center of Large Scale Reactor Engineering and Technology, Ministry of Education, State Key Laboratory of Chemical Engineering, East China University of Science and Technology, Shanghai, 200237, PR China. (e-mail: kkun@yahoo.cn).

H. F. Ma is with Engineering Research Center of Large Scale Reactor Engineering and Technology, Ministry of Education, State Key Laboratory of Chemical Engineering, East China University of Science and Technology, Shanghai, 200237, PR China. (e-mail: mark@ecust.edu.cn).

H. T. Zhang is with Engineering Research Center of Large Scale Reactor Engineering and Technology, Ministry of Education, State Key Laboratory of Chemical Engineering, East China University of Science and Technology, Shanghai, 200237, PR China. (e-mail: zht@ecust.edu.cn).

W. Y. Ying is with Engineering Research Center of Large Scale Reactor Engineering and Technology, Ministry of Education, State Key Laboratory of Chemical Engineering, East China University of Science and Technology, Shanghai, 200237, PR China. (Corresponding author to provide phone: +86 21 64252192; fax: +86 21 64252192; e-mail: wying@ecust.edu.cn).

D. Y. Fang is with Engineering Research Center of Large Scale Reactor Engineering and Technology, Ministry of Education, State Key Laboratory of Chemical Engineering, East China University of Science and Technology, Shanghai, 200237, PR China. (e-mail: dyfang@ecust.edu.cn).

of cobalt-based catalyst powder compacts, and found that the thermal conductivity of the catalyst specimens increases linearly with temperature and density and practically independent of the particle size of the powder in an atmosphere of air, while the porosity dependence of the thermal conductivity is inverse to that of density.

Dongsheng Wen et al. [12] have measured both radial and axial direction temperature distribution under the constant wall temperature conditions. Effective thermal conductivities and convective heat transfer coefficient have been derived based on the steady-state measurements and the two-dimensional axial dispersion plug flow (2DADPF) model.

Although one dream of some engineers and scientists may be that heat transfer results can be obtained for all systems through strictly numerical methods clearly that has not come to pass and probably never will. The need for experiments remains strong. Even with the success of numerical analysis, in solving conduction and laminar flow problems, calculations for turbulent and some separated flows still require experimental input for empirical constants and verification. Also one still needs thermodynamic and transport properties of materials for real problems and these unfortunately cannot be calculated accurately from first principles. Thus the need for measurements is clear, and measurements require sensors, data acquisition systems, and readout equipment. The development of better, simpler, and more accurate measurement techniques was the subject of the present section. This relates to experimental methods in heat transfer research and applications. These are the subcategories of the present section.

This paper aims principally to obtain more comprehensive experimental information of temperature field in the interior of a fixed bed including radial and axial temperature distribution, temperature difference between center and edge of the reactor and the effect of operating conditions on the temperature distribution. The simulation of a reactor for a strongly exothermic process based upon a model accounting for velocity and temperature profiles. The present work can provide reliable experimental data for the establishment of the two-dimensional pseudo-homogeneous heat transfer model.

II. EXPERIMENT

A. Experimental Apparatus

The apparatus had been designed, constructed and commissioned by local plant in our university as shown in Fig. 1. The internal diameter of the fixed bed reactor was 100 mm and the height was 500 mm, which was made of stainless steel and insulated externally with 10 mm vacuum layer and 200 mm glass wool, the sketch was showed in Fig. 2. The influence of fixed bed height on the effective radial thermal conductivity and the wall coefficient can be disregarded when the tube-to-particle diameter ratio $N > 100$. A 15mm copper rod with 10mm electrical heating pipe inside, with a $\Phi 3$ mm thermowell located in tangential position and through the wall of the copper rod, was inserted in the center of the fixed bed to provide stable heat source and accurate temperature. The

thermocouple can be inserted into the thermowell to monitor the wall temperature and kept the temperature uniform by connecting with the temperature control panel. There were 12 thermowells located at four radial positions of 25, 33.5, 45.5, and 48.5 mm from the reactor centerline. Axial temperature profile can be measured by the thermocouples located at six axial positions of 20, 80, 140, 200, 260 and 320mm from the inlet. At the same time, radial temperature profiles were obtained by these thermocouples in each of the axial position, where the thermocouples were located at the same section. The temperature measuring points of thermocouples on each bed section were shown in table I. Two steel gas distributing plates and two conical gas distributors were located on the both sides of the bed in order to guarantee the gas inlet and outlet was uniform distribution. The inlet air temperature was measured by a thermocouple located in the inlet of the main bed section.

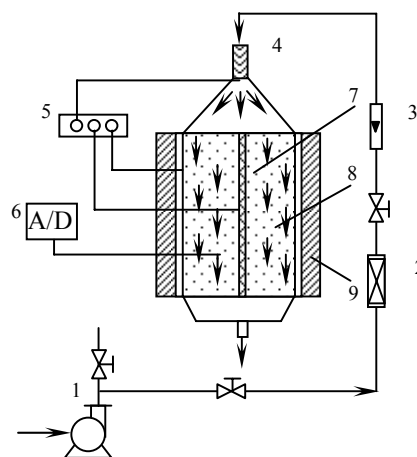


Fig. 1 Experimental flow sheet
1-Air compressor; 2-Dryer; 3- Rotameter; 4-Preheater;
5- Temperature controller; 6-Temperature demonstrator;
7-Heating pipe; 8-Catalyst; 9- Insulating layer

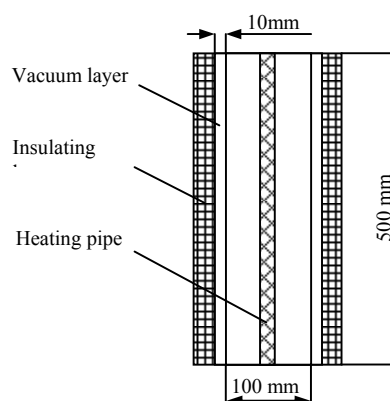


Fig. 2 Sketch of fixed-bed reactor

TABLE I
TEMPERATURE MEASURING POINTS OF THERMOCOUPLES ON EACH BED SECTION

Axial (Number)	Height (mm)	Measuring points			
		r1 (mm)	r2 (mm)	r3 (mm)	r4 (mm)
1	20	25	33.5	45.5	48.5
2	80	25	33.5	45.5	48.5
3	140	25	33.5	45.5	48.5
4	200	25	33.5	45.5	48.5
5	260	25	33.5	45.5	48.5
6	320	25	33.5	45.5	48.5

All temperature signals were collected by a data acquisition system and thermocouple amplifier was used to achieve high accuracy of temperature measurements. The heating pipe was provided by a three-zone ceramic heater controlled by an independent temperature control unit. Experiments were performed in steady states under different operating conditions.

All thermocouples were calibrated before use and were found to have an accuracy of 0.1°C. Heat conduction through the stainless-steel supporting rod and arms was found to be small due to high tube-to-particle diameter ratio N . As the temperature was not very high, the radiation effect can be neglected. The uncertainties of air flow rate under the conditions of this work were estimated to be 3% [13].

B. Experiment Procedure

The test bed was packed by pouring commercial methanol synthesis catalyst of $\Phi 5 \times 5$ mm into it in a random manner and compressed air was passed through the bed to simulate the flow condition of the actual reaction process.

In Fig. 1 we illustrated the flow sheet of experimental procedure. The air supplied by a compressor first passed through the oil filter and the silica gel dryer, then the stable and clean compressed air passed through the pressure regulating valve, its flow rate was monitored by a glass rotameter and controlled by a flow controller, an electric preheater, connected to a temperature controller, heated the air to the desired temperature before introducing it into the fixed-bed. After transmitted heat with the fixed bed, the air outlet was vented directly.

C. Experiment Condition

The experiment was carried out with the range of air volumetric flow rate 2~8 m³/h, inlet air temperature 160~200°C, heating pipe temperature 210~270°C. The experimental measuring points were arranged in accordance with the orthogonal experimental design.

It normally took about three hours (depending on the gas flowrate) from the cold to reach the steady state when the temperature profile in the packed bed did not change with time. For every experimental condition three replicas were made.

III. RESULTS AND DISCUSSION

A. Axial Temperature Distribution

The experimental conditions were as follows: inlet air temperature $t_{in}=160^\circ\text{C}$, heating pipe temperature $t_w=255^\circ\text{C}$, air volumetric flow rate $G=5\text{m}^3/\text{h}$. The steady-state temperature in the fixed bed at different radial position was plotted as a function of axial position in Fig. 3.

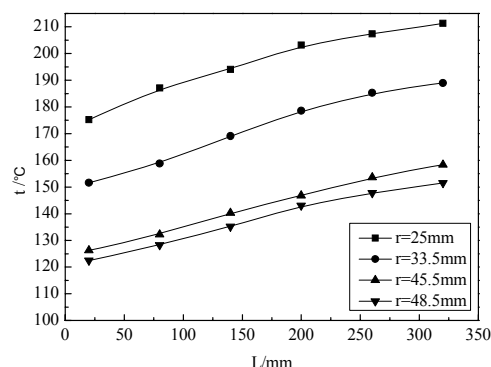


Fig. 3 Steady-state axial temperature distribution

The axial temperature distribution showed in Fig. 3 had a similar trend at different radial position. It can be seen that at given operating conditions, the temperature increased monotonically with axial distance increasing. As known that if $G=0\text{m}^3/\text{h}$, the curve of axial temperature distribution within the fixed bed should be a straight line, and temperature gradient would not exist anymore, this was consistent with the reported literature [14]. When the air flowed through the fixed bed and the air temperature was not too high, the inlet gas played a role in cooling the bed, its temperature increased while passing through the fixed bed. The higher the gas temperature reached, the quantity of heat took from the fixed bed was relatively reduced, this due to the axial temperature distribution showed in Fig. 4.

B. Radial Temperature Distribution

The experimental conditions were as follows: inlet air temperature $t_{in}=170^\circ\text{C}$, heating pipe temperature $t_w=210^\circ\text{C}$, air volumetric flow rate $G=2\text{m}^3/\text{h}$. The radial temperature distribution at the steady state was shown in Fig. 4 for the six different axial positions, where the dashed lines represent the position of the inner wall surface of the copper rod.

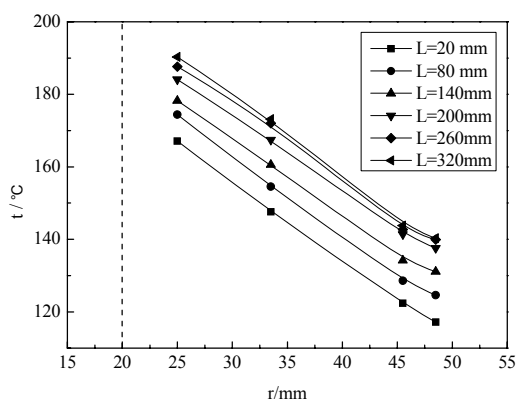
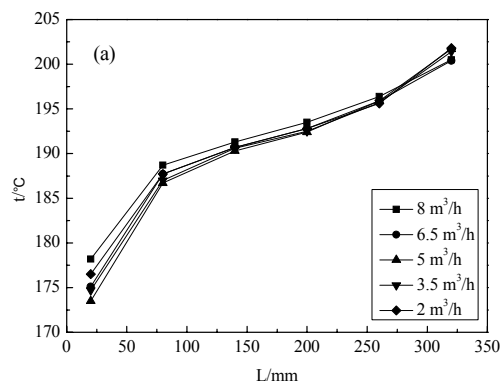


Fig. 4 Steady-state radial temperature distribution

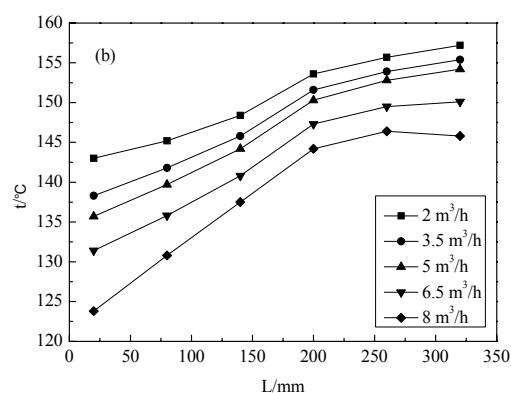
The curves of radial temperature distribution at different height were similar to each other. For a given axial section, the temperature distribution depends on the height from the inlet, farther away from the inlet, the higher temperature was obtained. In Fig. 4, it can be seen that the temperature at the position of $r=25\text{mm}$ was lower than the heating pipe temperature and there was a large temperature drop from the center to the inner wall of the reactor. With the radius increasing, the radial temperature decreased rapidly, this phenomenon mainly due to the internal thermal resistance. The larger the radius reached, the greater the thermal resistance of the bed increased, and the radial effective thermal conductivity decreased, the heat quantity cannot be transmitted efficiently, then the temperature drop appeared.

C. Effects of the Air Flow Rate G

The experimental conditions were as follows: inlet air temperature $t_{in}=180^\circ\text{C}$, heating pipe temperature $t_w=240^\circ\text{C}$, air volumetric flow rate $G=2\sim 8\text{m}^3/\text{h}$. The axial temperature distribution at the steady state was shown in Fig. 5 for the five different flow rates. Fig. 5(a), $r=25\text{mm}$; Fig. 5(b), $r=45.5\text{mm}$. The curve type was corresponding to the reported literature [15-16]. The radial temperature distribution at the steady state was shown in Fig. 6 for the five different air volumetric flow rates, where the dashed lines represent the position of the inner wall surface of the copper rod. Fig. 6(a), $L=80\text{mm}$; Fig. 6(b), $L=260\text{mm}$.



(a)

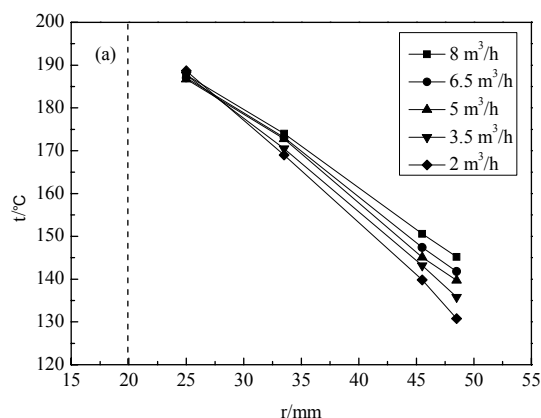


(b)

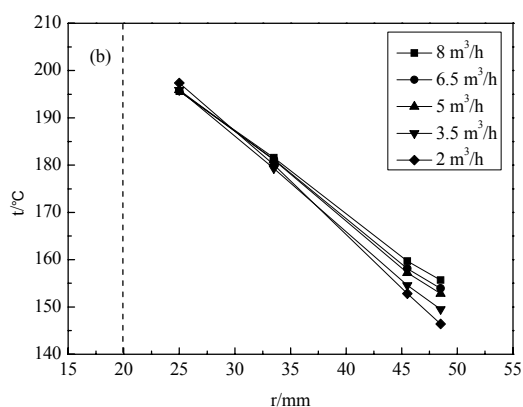
Fig. 5 (a) Effect of flow rate on axial temperature distribution ($r=25\text{mm}$) (b) Effect of flow rate on axial temperature distribution ($r=45.5\text{mm}$)

A comparison between Fig. 5(a) and Fig. 5(b) indicates that the non-uniformity of the axial temperature distribution increased with air volumetric flow rate increasing. In Fig. 5(a), there was a unusual phenomenon that the temperature curves almost overlapped with each other, this was mainly due to the heat supplied by the heating pipe was far more than the heat removed by the air. The temperature distribution of the position $L=20\&320\text{mm}$ did not line to this law, that because the heat loss was inevitable at the inlet and outlet of the reactor. Scilicet, in the vicinity of the heating pipe, the effect of flow rate on temperature was slight even negligible. In Fig. 5(b), it can be seen that the distribution was S-shaped for all air flow rate other than $2\text{m}^3/\text{h}$. For a given flow rate, the temperature increased with axial distance increasing slowly first at $L < \sim 150\text{mm}$, then rapidly at $L=150\sim 250\text{mm}$, and finally slowly again at $L > \sim 250\text{mm}$. Fig. 5(b) also represented a temperature drop at the vicinity of the outlet at $2\text{m}^3/\text{h}$. The temperature drop was firstly due to the low flow rate that the air could not transmit the heat promptly and secondly due to the heat losses from the bed outlet which was inevitable. As models for heat transfer in packed beds often lump the flow rate into the effective wall-fluid heat transfer coefficient, the above results suggest

that the heat transfer coefficient be a function of the flow rate.



(a)



(b)

Fig. 6 (a) Effect of flow rate on radial temperature distribution (L=80mm) (b) Effect of flow rate on radial temperature distribution (L=260mm)

Fig. 6 indicated the effect of the air volumetric flow rate on the radial temperature distribution. At the position of $r=25\text{mm}$, $L=320\text{mm}$, the temperature increased slightly with the flow rate increasing, take many factors into consideration, such as measurement error, the temperature at this position can be considered invariant, this result corresponding to the previously obtained conclusion. With the radius increased, the effect of flow rate became prominently, this was mainly due to the internal thermal resistance of the bed. The larger the radius reached, the greater the thermal resistance of the bed, and the lower temperature appeared. Depending on the heat transfer rate equations (1) and (2), α_1 is a function of Reynolds number, while Reynolds number is a function of the flow rate, so K increased with the flow rate increasing, that why the radial temperature distribution increased with the flow rate increasing.

$$Q = KA\Delta t_m \quad (1)$$

In the equation,

Q - Heat transfer quantity;

K - Total heat transfer coefficient;

A - Heat transfer area;

Δt_m - Mean temperature difference.

$$\frac{1}{K} = \frac{1}{\alpha_1} + \frac{1}{\alpha_2} + \frac{\delta}{\lambda} + R \quad (2)$$

In the equation,

α_1, α_2 - cold/thermal fluid heat transfer coefficient, $W/(m^2 \cdot K)$;

λ - Thermal conductivity of wall, $W/(m \cdot K)$;

δ - Pipe wall thickness, m;

In conclusion, the temperature at radial positions other than the heating pipe vicinity increased with the flow rate increasing, and the increasing rate increased as the radius increasing. Under different air volumetric flow rates, temperature decreased at different rates. The increase of flow rate facilitated heat transfer in the fixed bed.

D. Effect of Inlet Air Temperature t_{in}

The experimental conditions were as follows: inlet air temperature $t_{in}=160\sim 200^\circ\text{C}$, heating pipe temperature $t_w=240^\circ\text{C}$, air volumetric flow rate $G=3.5\text{m}^3/\text{h}$. The axial temperature distribution at the steady state was shown in Fig. 7 for the five different inlet air temperatures, and the radial temperature distribution at the steady state was shown in Fig. 8 for the five different inlet air temperatures, where the dashed lines represent the position of the inner wall surface of the copper rod. Fig. 7, $r=45.5\text{mm}$; Fig. 8, $L=260\text{mm}$.

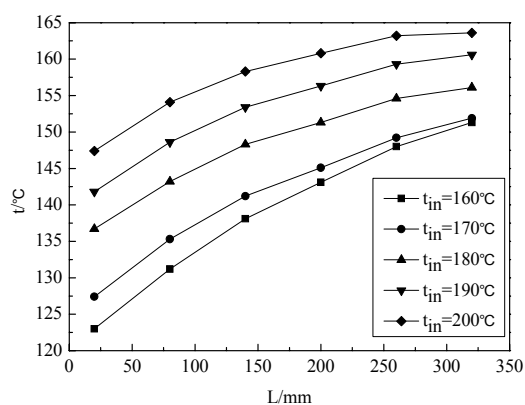


Fig. 7 Effect of t_{in} on axial temperature distribution

Fig. 7 indicated that the average temperature of the fixed bed increased with the inlet air temperature increasing, but the temperature difference between the reactor outlet and inlet decreased with the inlet air temperature increasing. When the other experimental conditions remained unchanged, with the inlet air temperature increasing, the difference between t_{in} and t_w becoming smaller, heat transfer quantity Q carried by a

certain amount of gas from the upper part reducing, the following section of the bed did not have enough Q to elevate its temperature to higher level. For these reasons, with the increasing of the inlet air temperature, the axial temperature increasing rate would slow down and the distribution would tend to a line distribution at last.

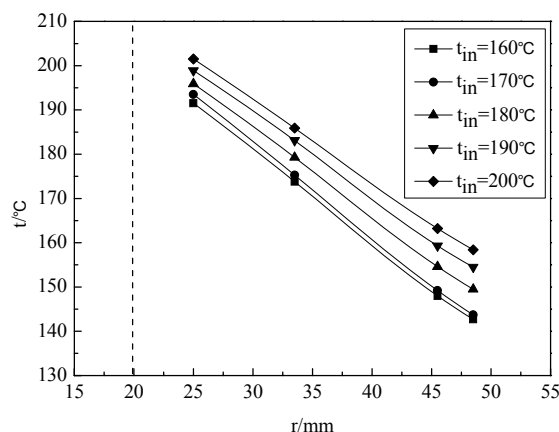


Fig. 8 Effect of t_{in} on radial temperature distribution

Fig. 8 showed that the average temperature of the bed at the position of $L=260\text{mm}$ increased with the inlet air temperature increasing. Different with the influence of the gas flow rate, the temperature in the vicinity of the heating pipe changed with the inlet air temperature, this results firstly due to the higher inlet air temperature of the flowing air that could contain more heat quantity Q , and the cross sections of the bed can get more Q to improve the temperature; Secondly, with the inlet air temperature increasing, the internal thermal resistance of the fixed bed become bigger (with t_{in} increasing, the Reynolds number increasing, K decreasing, then the internal thermal resistance increasing), the effect of the heating pipe in this area ($r=25\text{mm}$) was not great any more.

E. Effect of Heating Pipe Temperature t_w

The experimental conditions were as follows: inlet air temperature $t_{in}=180^\circ\text{C}$, heating pipe temperature $t_w=210\sim 270^\circ\text{C}$, air volumetric flow rate $G=3.5\text{m}^3/\text{h}$. The axial temperature distribution at the steady state was shown in Fig. 9 for the five different heating pipe temperatures, and the radial temperature distribution at the steady state was shown in Fig. 10 for the five different heating pipe temperatures, where the dashed lines represent the position of the inner wall surface of the copper rod. Fig. 9, $r=45.5\text{mm}$; Fig. 10, $L=260\text{mm}$.

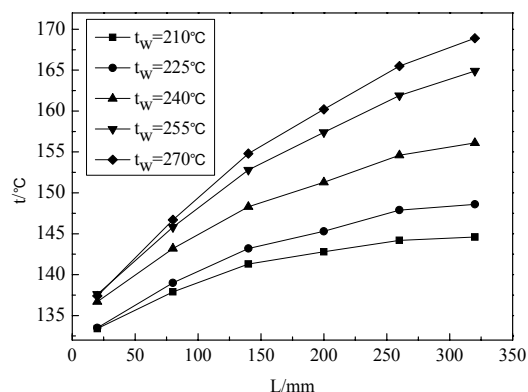


Fig. 9 Effect of t_w on axial temperature distribution

Fig. 9 illustrated the effect of heating pipe temperature on the axial temperature distribution. By increasing the heating pipe temperature, which caused the average temperature of the fixed bed increased, and the temperature differences between outlet and inlet also increased. As shown in Fig. 9 the higher the heating pipe temperature, the greater influence on axial temperature distribution. With the other experimental conditions remain unchanged, when the heating pipe temperature increasing, the more quantity heat which produced by the heating pipe can be brought to the following section by the flowing air in a unit time, then the temperature of these positions increased. While $t_w < \sim 225^\circ\text{C}$, $t_{in}=180^\circ\text{C}$, the heat transfer quantity supplied by the heating pipe less than the heat quantity removed by the inlet gas, the area $L < 50\text{mm}$ was heated by the inlet gas, that why the effect of heating pipe temperature was not obvious; while $t_w > 255^\circ\text{C}$, the temperature difference between t_w and t_{in} was increased, the effect was gradually emerging, increased the heating pipe temperature was not conducive to the axial temperature distributed uniformly.

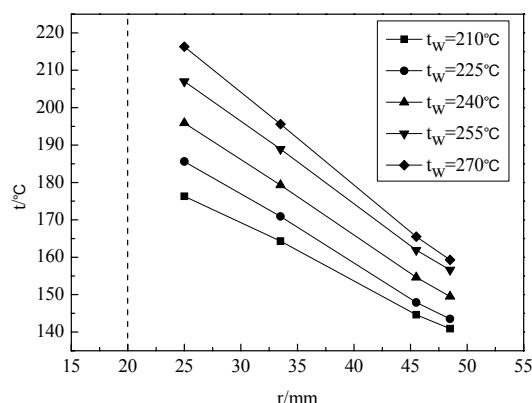


Fig. 10 Effect of t_w on radial temperature distribution

Fig. 10 illustrated the effect of heating pipe temperature on the radial temperature distribution. With the heating pipe temperature increasing, the average temperature of the fixed

bed obviously increased, especially in the area near the heating rods, where the temperature increased conspicuously. While the other experimental conditions were kept constant, with the heating pipe temperature increasing, the more heat quantity which produced by the heating pipe could be brought to the fixed bed, then the temperature of the bed at the radial position automatically increased. However with the radius increasing, the thermal resistance of the bed also increased rapidly and reached the maximum at the edges of the bed, the heat provided by the heating pipe might not well be transmitted to the edge of the bed, which cause the effect of heating pipe temperature was not conducive to the radial uniform temperature distribution. The effect of heating pipe temperature on the center area of the bed was stronger than outer edge of the bed. In conclusion, if the heating pipe temperature was too high, it will cause the temperature difference between center area and outer edge of the bed at cross sections too large, which was not conducive to the uniform temperature distribution of the bed and the stable operation of the fixed bed.

IV. CONCLUSIONS

The steady-state heat transfer behavior of a gas flowing through a fixed bed had been investigated experimentally. Both radial and axial direction temperature distribution had been measured under the different operating conditions.

(1) The experiment was carried out in a fixed bed with the range of inlet air temperature 160~200°C, heating pipe temperature 210~270°C and air flow rate 2~8m³/h. The temperature distribution shown that the axial temperature increased monotonically with height increasing, and radial temperature decreased with the radius increasing.

(2) Operating conditions had a significant impact on the fixed bed that the temperature of arbitrary position in the fixed bed increased with the increasing of air flow rate, inlet air temperature or the air flow rate. The experimental results showed that a higher inlet air temperature was conducive to a uniform distribution in the fixed bed. There was a large temperature drop existed at the radial direction, and the temperature drop increased with the heating pipe temperature increasing. A higher air flow rate can improve the heat transfer in the fixed bed.

The thermal distribution would affect the reaction rate, the heat storage and release rate, energy storage devices, thermal efficiency and other aspects, therefore, studied the temperature distribution in the fixed bed had a great significance. Based on the thermal distribution, heat transfer models of the fixed bed could be established, and the characteristics of the temperature distribution in the fixed bed could be finely described, that had an important practical significance.

NOMENCLATURE

G— air volumetric flow rate, m³/h
L— the height from the inlet, mm
N— tube-to-particle diameter ratio

r — radius, mm

t_{in} — inlet air temperature, °C

t_w — heating pipe temperature, °C

ACKNOWLEDGMENT

The authors acknowledge financial support in this research from the National Key Technology R&D Program of China (No. 2006BAE02B02).

REFERENCES

- [1] K. C. Xie, D. Y. Fang, Methanol technology, Beijing: Chemical Industry Press, 2010
- [2] H. F. Ma, W. Y. Ying, D. Y. Fang, "Simulation of a combined converter for methanol synthesis", *Journal of east China University of Science and Technology*, vol. 34, no. 2, pp. 149-153, 2008
- [3] R. Caulkin, A. Ahmad, M. Fairweather, X. Jia, R. A. Williams, "An investigation of sphere packed shell-side columns using a digital packing algorithm". *Computers and Chemical Engineering*, vol. 31, no.12, pp. 1715-1724, December. 2007
- [4] A. Cybulski, J. A. Moulijn, Structured catalysts and reactors, New York: Marcel Dekker Inc, 2th, pp. 1-18, 1998
- [5] H. Freund, T. Zeiser, F. Huber, E. Klemm, G. Brenner, F. Durst, G. Emig, "Numerical simulations of single phase reacting flows in randomly packed fixed-bed reactors and experimental validation", *Chemical Engineering Science*, vol. 58, no. 3-6, pp. 903-910, February–March. 2003
- [6] S. S. Bertsch, E. A. Groll, S. V. Garimella, "A composite heat transfer correlation for saturated flow boiling in small channels", *International Journal of Heat and Mass Transfer*, vol. 52, no7-8, pp. 2110-2118, March. 2009
- [7] A. G. Dixon, G. Walls, H. Stanness, M. Nijemeisland, E. H. Stitt, "Experimental validation of high Reynolds number CFD simulations of heat transfer in a pilot-scale fixed bed tube", *Chemical Engineering Journal*, vol. 200-202, pp. 244-256, 15 August. 2012
- [8] A. Guardo, M. Coussirat, F. Recasens, M. A. Larrayoz, X. Escaler, "CFD study on particle-to-fluid heat transfer in fixed bed reactors: Convective heat transfer at low and high pressure", *Chemical Engineering Science*, vol. 61, no. 13, pp. 4341-4353, July. 2006
- [9] H. P. A. Calis, J. Nijenhuis, B. C. Paikert, F. M. Dautzenberg, C. M. van den Bleek, "CFD modelling and experimental validation of pressure drop and flow profile in a novel structured catalytic reactor packing", *Chemical Engineering Science*, vol. 56, no. 4, pp. 1713-1720, February. 2001
- [10] J. Xu, W. S. Wei, A. Z. Tian, Y. Fan, X. J. Bao, C. C. Yu, "Temperature profile in a two-stage fixed bed reactor for catalytic partial oxidation of methane to syngas", *Catalysis Today*, vol. 149, no. 1-2, pp. 191-195, 15 January. 2010
- [11] J. M. Wu, H. T. Zhang, W. Y. Ying, D. Y. Fang, "Thermal conductivity of cobalt-based catalyst for Fischer–Tropsch synthesis", *International journal of thermophysics*, vol. no. 3, pp. 556-571, March. 2010
- [12] D. S. Wen, Y. L. Ding. "Heat transfer of gas flowthrough a packed bed", *Chemical Engineering Science*, vol. 61, no. 11, pp. 3532-3542, June. 2006
- [13] Y. L. Ding, Z. L. Wang, D. S. Wen, M. Ghadiri, X. F. Fan, D. Parker, "Solids behaviour in a gas–solid two-phase mixture flowing through a packed particle bed", *Chemical Engineering Science*, vol. 60, no. 19, pp. 5231-5239, September. 2005
- [14] C. A. Coberly, W. R. Marshall. "Temperature gradients in gas streams flowing through fixed granular beds", *Chemical Engineering Progress*, vol. 47, pp. 141-147, 1951
- [15] A.P. de Wasch, G.F. Froment, "Heat transfer in packed beds", *Chemical Engineering Science*, vol. 27, no. 3, pp. 567-576, March. 1972
- [16] A. G. Dixon, W. R. Paterson. "Heat transfer in packed beds of low tube/particle diameter Ratio", Houston: ACS Publications, pp. 238-253, 1978